

www.acsabm.org Article

Self-Patterned Nanoscale Topography of Thin Copolymer Films Prepared by Evaporative Assembly-Resist Early-Stage Bacterial Adhesion

Jiachun Shen, Danielle Guercio, Ilana L. Heckler, Ting Jiang, Scott T. Laughlin, Elizabeth M. Boon, and Surita R. Bhatia*



Cite This: ACS Appl. Bio Mater. 2022, 5, 3870-3882



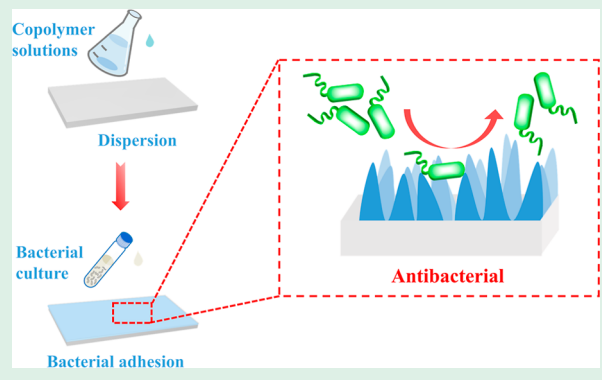
ACCESS I

III Metrics & More

Article Recommendations

Supporting Information

ABSTRACT: Biofilm formation on the surfaces of indwelling medical devices has become a growing health threat due to the development of antimicrobial resistance to infection-causing bacteria. For example, ventilator-associated pneumonia caused by *Pseudomonas* and *Staphylococci* species has become a significant concern in treatment of patients during COVID-19 pandemic. Nanostructured surfaces with antifouling activity are of interest as a promising strategy to prevent bacterial adhesion without triggering drug resistance. In this study, we report a facile evaporative approach to prepare block copolymer film coatings with nanoscale topography that resist bacterial adhesion. The initial attachment of the target bacterium *Pseudomonas aeruginosa* PAO1 to copolymer films as well as homopolymer films was evaluated by fluorescence microscopy. Significant reduction in bacterial adhesion



(93–99% less) and area coverage (>92% less) on the copolymer films was observed compared with that on the control and homopolymer films [poly(methacrylic acid) (PMAA)—only 40 and 23% less, respectively]. The surfaces of poly(styrene)-PMAA copolymer films with patterned nanoscale topography that contains sharp peaks ranging from 20 to 80 nm spaced at 30–50 nm were confirmed by atomic force microscopy and the corresponding surface morphology analysis. Investigation of the surface wettability and surface potential of polymer films assists in understanding the effect of surface properties on the bacterial attachment. Comparison of bacterial growth studies in polymer solutions with the growth studies on coatings highlights the importance of physical nanostructure in resisting bacterial adhesion, as opposed to chemical characteristics of the copolymers. Such self-patterned antifouling surface coatings, produced with a straightforward and energy-efficient approach, could provide a convenient and effective method to resist bacterial fouling on the surface of medical devices and reduce device-associated infections.

KEYWORDS: biofilm formation, Pseudomonas aeruginosa, antifouling, surface topography, surface roughness

INTRODUCTION

Bacterial infections associated with the application of medical and implant devices have been recognized as one of the public health challenges that could cause biomedical device failure and severe complications to patients. 1,2 For example, common Gram-negative pathogens including Pseudomonas and Staphylococci species are the main contributors to ventilatorassociated pneumonia, which may become a severe threat, especially during the COVID-19 pandemic.³ The prevalence of device-associated infections could be ascribed to the adhesion of pathogenic bacteria to the abiotic or biotic surface of biomaterials, which results in the development of biofilms. Biofilms are microbial communities enclosed by self-secreted extracellular polymeric substances.^{4,5} The complex composition and robust structure of biofilms, as well as changes in bacterial metabolism and gene expression, result in ~1000-fold greater resistance to antibiotic treatments and host immune

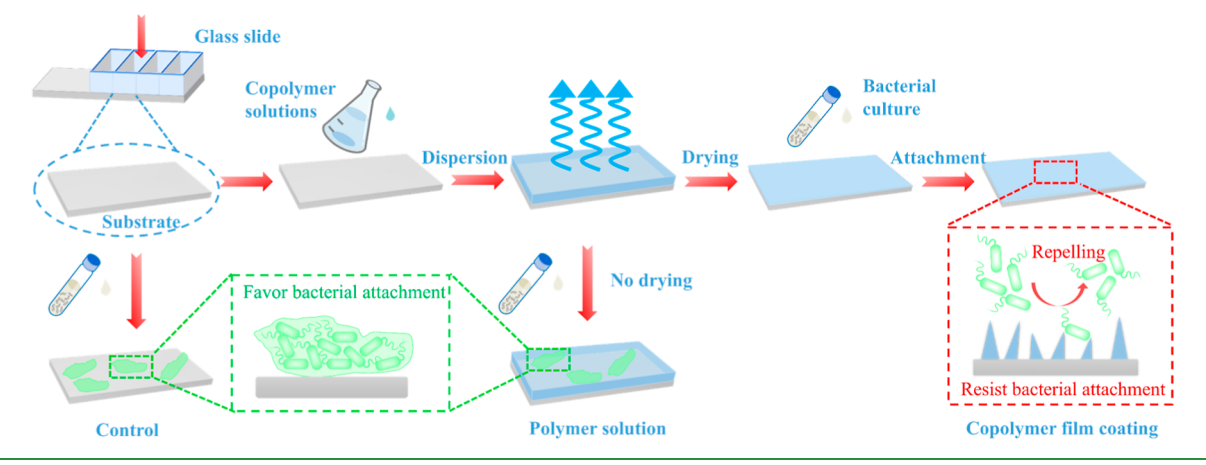
responses than the same bacteria in the planktonic form; bacteria deeper in the biofilm are especially protected.^{6,7} Thus, treatment of biofilms typically requires an increasing dosage of antibiotics over time, and this inevitably leads to the development of antibiotic resistance.⁸ According to the U.S. Center for Disease Control and Prevention (CDC), antibiotic-resistant infections lead to more than 2.8 million cases in the United States with more than 35,000 deaths every year.⁹ Preventing biofilm formation would be the most effective method of treatment of device-associated infections. Thus,

Received: May 2, 2022 Accepted: July 12, 2022 Published: July 27, 2022





Scheme 1. Schematic Illustration of the Preparation of Thin Copolymer Films for Resisting Bacterial Attachment



development of methods to control and eliminate the biofilm before the occurrence of infections is imperative.

Considering that bacterial adhesion is the critical first step for biofilm formation, inhibition of bacterial adhesion is an attractive approach to the prevention of surface biofouling. 10-12 Currently, there are several proposed approaches to create such an antibacterial surface. One of these methods is to chemically modify the material surface with the functionalization or immobilization of various antimicrobial agents, including metal nanoparticles, ¹³⁻¹⁵ antimicrobial compounds, ¹⁶⁻¹⁸ and quaternary ammonium compounds. ^{19,20} For example, Yang and coworkers functionalized the polyvinyl chloride surface with an antioxidant precursor N-acetylcysteine by plasma immersion ion implantation treatment, and this caused significant reduction in biofilm viability for both Grampositive and Gram-negative bacteria.¹⁷ Chen et al. studied the effect of surface-tethered functional peptides with different poly(ethylene oxide) (PEO) chain lengths on cell behaviors and found that the medium-length PEO assisted the functional peptides to achieve optimal antifouling behavior.²¹ However, such techniques may be compromised due to the limited duration of effectiveness and the uncontrolled release of antibacterial substances. There are also concerns about the potential of these toxic bactericidal compounds or nanoparticles to negatively affect the human health.²² In order to tackle these challenges, antifouling surfaces that provide physical barriers to bacterial adhesion, rather than chemical bactericidal agents, have been put forward. Inspired by naturally occurring surfaces of cicada insects, 23,24 shark skin, 25 or lotus leaves, 26,27 surfaces with micro- or nanoscale roughness have gained interest as a means to prevent bacterial fouling. 12,28-33 This provides an efficient and enduring strategy to resist bacterial adhesion on the surface, which is independent of the surface chemistry.

Extensive studies have been carried out since Ivanova et al. first reported the excellent bactericidal properties exerted by nanopillars on the wings of cicada insects when treating the pathogenic bacterium *Pseudomonas aeruginosa*.²³ It was found that such nanopillar structures on the surface could alter and penetrate the bacterial cell membranes by direct contact and cause significant damage by mechanical bactericidal action. Upon modifying the surface chemistry with gold coatings, similar surface topography and bactericidal ability were retained, which indicates that the antibacterial effect originates from the physical interactions with bacteria. This has led to

additional studies focusing on a series of bactericidal nanotopographies, including nanopillars, ^{10,34,35} nanocones, ^{32,36} and other biomimetic nanostructures, ^{26,37,38} which mostly explored the effects of physico-mechanical features on bacteria without the addition of chemical antimicrobial compounds to the surfaces. For example, Jiang et al. ²⁶ designed a hierarchically structured silicon surface based on a lotus leaf with nanoneedle tips around 30–50 nm that repelled more than 99% of bacteria and displayed durable mechanical bactericidal activity. Linklater et al. ³⁴ reported that densely packed nanopillars of black silicon with heights of 280 nm effectively killed Gram-negative bacteria by potential membrane rupture. Additionally, Cao et al. ²⁹ fabricated hierarchical surface replicas of rose petals with microscale papillae and nanoscale cuticular folds, which successfully delayed initial bacterial cell attachment and biofilm formation.

However, these well-designed surface topographies with ordered patterns or artificial biomimetic surfaces require sophisticated fabrication procedures, significant energy consumption, and often involve harsh reaction conditions including an etching or a curing process. 22,39 These techniques include nanoimprint or UV lithography, 26,33 reactive ion etching, 40 chemical vapor deposition, 32 nanotemplating, 10 and so on. It is desirable to obtain nanoscale patterned surfaces by a facile and cost-saving approach without compromising the bactericidal capacity. Additionally, numerous studies focus on surfaces that are inorganic materials including titanium, aluminum, and silicon wafers; relatively fewer studies have explored surfaces composed of nanotextured synthetic polymer films, in spite of the fact that polymer materials and coatings are widely used in biomedical devices. Previous studies have revealed that topographic modifications with polymer coatings could also significantly affect the initial bacterial attachment and hinder the subsequent development of biofilms. Kargar et al.³¹ found that the close-packed layer of 630-1550 nm colloidal polystyrene spheres effectively reduced more than 80% of attached P. aeruginosa and inhibited the colony formation, while the 220 nm colloidal particle surface maintained much higher colony density. They also found that P. aeruginosa may prefer the specific location on the larger colloidal particle surface where colony formation may be restricted due to less possibility for cell communication.¹² Cui et al.¹⁰ fabricated the ordered conical polycarbonate nanostructured surface that showed effective inactivation of Escherichia coli attachment

with the critical height of nanopillars around 200 nm. However, there has been some work to identify whether there are chemical characteristics of polymeric films that may promote the resistance to bacterial adhesion. For example, Lu et al. 14 reported that hydrogel thin films consisting of a series of poly(2-alkylacrylic acid) copolymers fabricated using a layer-by-layer approach exhibited increasing antibacterial functionality with increasing hydrophobicity of hydrogel films to *Staphylococcus epidermidis*, which may be due to the penetration of hydrophobic polymer segments into the bacterial membrane.

Hence, the present study provides a facile approach to prepare thin polymer films with self-patterned nanoscale structures on the surface with block copolymers such as poly(styrene)-b-poly(methacrylic acid) (PS-PMAA), poly-(styrene)-b-poly(acrylic acid) (PS-PAA), and poly(styrene)b-poly(ethylene oxide) (PS-PEO), as shown in Scheme 1. The prepared polymer films were evaluated for potential bacterial resistance with P. aeruginosa as the target bacterium. The homopolymer films of PMAA and poly(methyl methacrylate) (PMMA) were also examined for comparison. Fluorescence microscopy revealed significant differences in bacterial attachment between the homopolymer and copolymer films. The nanoscale features in the surface morphology of the polymer films were verified by atomic force microscopy (AFM) and the corresponding topographical parameters were analyzed. Examination of surface wettability and surface potential was also carried out to explore the relationship between the bacterial resistance and surface properties. It was confirmed that physical nanoscale structures on the copolymer film surface, and not simply the presence of polymers, were responsible for antifouling activity by comparing bacterial attachment on substrates coated with polymer films to samples in which bacterial cultures were directly dispersed in polymer solutions. We believe this method provides a convenient approach to fabricating antifouling surfaces, which is free of any complex fabrication process and provides novel insights into the design of antibacterial surfaces by synthetic polymers, which may have great potential in the application of antibacterial coatings.

MATERIALS AND METHODS

General Materials. PS-PMAA ($M_{\rm n}$: 3000:22,300), PS-PAA ($M_{\rm n}$: 3500:23,000), and PS-PEO ($M_{\rm n}$: 3600:16,600) were purchased from Polymer Source Inc (Canada). PMMA powder (size: 600 μ m, $M_{\rm w} \sim 550,000$ g/mol) was purchased from Thermo Fisher Scientific (USA). Sodium salt solution of PMAA (40 wt %, $M_{\rm w}$: 4000–6000 g/mol) was obtained from Sigma-Aldrich (USA) (polymer structures are provided in Figure S1). Acetonitrile, acetone, and ethanol were purchased from Fisher Scientific (USA). All chemicals were used without any further treatment. The four-well glass chamber slides (Lab-Tek II Chamber Slide System, glass substrate with a removable polystyrene chamber, growth area: 1.7 cm², volume: 1 mL) were obtained from Fisher Scientific (USA). The plasmid pMF230 was a gift from Michael Franklin (Addgene, plasmid #62546).

Polymer Film Preparation. First, a specific amount of polymer powder or solution was measured and added to the corresponding solvent to prepare 4 wt % polymer solutions. For example, PS-PEO and PS-PMAA powder were added into water/acetone solution (v/v, 1:1.1) to prepare 4 wt % polymer solutions, respectively, while PMMA powder was dissolved in acetone. PS-PAA solution was obtained by dissolving polymer powder in a water/ethanol mixed solution (v/v, 1:1). For PMAA, the original aqueous solution was diluted by water/acetonitrile solution (v/v, 2.4:1) to make the polymer solution. Polystyrene colloid solutions were also applied, but

no robust or complete films were obtained. In this case, results are not presented.

Then, the obtained samples were sealed in vials and heated in the oven at 60 °C for 30 min to assist the dissolution. The obtained solutions were equilibrated for 24 h at room temperature to make sure all polymer powder dissolved and no bubbles existed. To make the thin polymer films, 150 μ L of polymer solution was added into the first three wells of chamber slides to make sure the glass substrate was fully covered by the polymer solution. The fourth well was intended to leave blank as the control. The chamber slides were placed in the fume hood overnight at room temperature. The thin polymer films were obtained after the complete evaporation of solvents, and no breakage was observed for the test samples. After the preparation, the films were covered to avoid potential wetting or contamination. For the experiment without the film predeposition, the same amount of polymer solution was dispersed into chamber slides without any further evaporation process before the bacterial attachment assay. In order to do the AFM and Kelvin probe force microscopy (KFM) measurements, polymer films were prepared with the same procedures except by using the silicon wafer instead of the glass substrate. For water contact angle (WCA) measurements, the wall of the chamber slide was removed and the glass substrate with thin films was reserved and used for the test.

Polymer Film Characterization. The surface morphology of the thin polymer films was characterized by using an atomic force microscope (Dimension Icon, Bruker) with the silicon wafer as a substrate. The surface potential profiles of polymer films were obtained on KFM mode with the SCM-PIT probe. Microscopic images were scanned at the scale of 5 μ m and the frequency of 0.5 Hz where height, phase, and potential channels were captured simultaneously. AFM and KFM images were processed and analyzed using Bruker NanoScope Analysis software (version 1.9). The obtained topographical data were processed with first-order leveling before analysis. Surface morphology parameters including surface roughness, skewness, surface area difference, height profile, and peak distributions were obtained.

Zeta potential measurements of the corresponding polymer solutions were performed with five repeats at 25 $^{\circ}$ C on the NanoBrook Omni instrument (Brookhaven Instrument Inc., Holtsville, NY).

Static WCAs of polymer films were measured using the DataPhysics contact angle analyzer (OCA 15 EC). A 10 μ L drop of deionized water was dropped onto the film. The contact angle was measured 20 s after the drop casting to ensure the water droplet reached equilibrium.

Bacterial Culture Conditions. Wild-type *P. aeruginosa* (*P. aeruginosa*) was transformed with pMF230, a plasmid that constitutively expresses green fluorescent protein (GFP). The plasmid also contains an ampicillin resistance cassette needed to provide antibiotic pressure to ensure retention of the plasmid. Carbenicillin was used instead of ampicillin as *P. aeruginosa* is highly resistant to ampicillin. We grew a shaking overnight culture of *P. aeruginosa* in Lennox Broth supplemented with $100~\mu g/mL$ carbenicillin at $37~^{\circ}C$. The minimal media used was M63. Media was prepared sterile using $22~mM~KH_2PO_4$, $40.2~mM~K_2HPO_4$, $15.1~mM~(NH_4)_2SO_4$, $1~mM~MgSO_4$, and 23~mM~arginine.

Bacterial Attachment Assay. 1 mL of overnight culture was diluted in 9 mL of minimal media M63 supplemented with $100~\mu g/$ mL carbenicillin to a final OD₆₀₀ of 0.3. We determined that there are 4.8×107 cells/mL at an OD₆₀₀ of 0.3 using CFU counting following a previously described method. To perform the bacterial adhesion assay, $500~\mu$ L of the diluted bacterial culture was added into each of the four chambers of the glass slide. The slides were incubated at 37 °C for 15 min to allow for bacterial attachment. After 15 min of incubation, each chamber of the slide was washed with $500~\mu$ L of M63 three times to remove unattached cells before imaging. To perform the bacterial attachment assay in the presence of a polymer solution, $500~\mu$ L of the diluted bacterial culture was added into each of the four chambers of the glass slide which contained the polymer solution. Bacterial attachment was evaluated using a Zeiss Axio

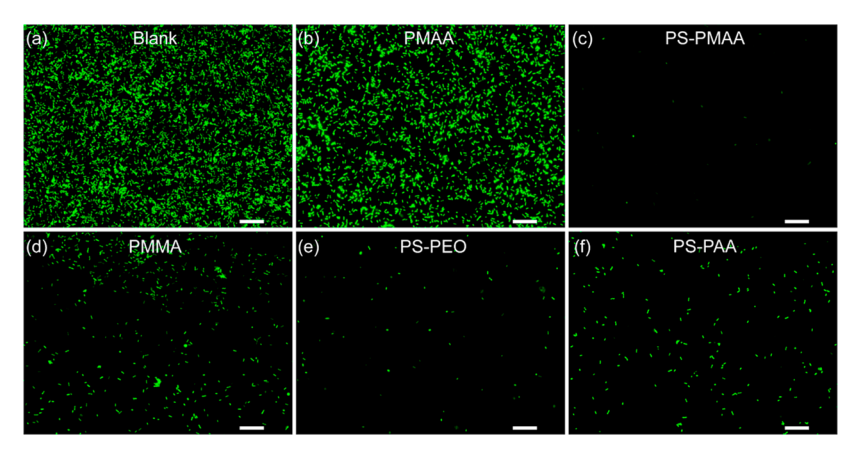


Figure 1. Representative fluorescence images of *P. aeruginosa* on the control and different polymer film surfaces: (a) blank, (b) PMAA, (c) PS-PMAA, (d) PMMA, (e) PS-PEO, and (f) PS-PAA. Scale bar: 20 μ m.

Vert.A1 inverted epifluorescence microscope equipped with a Lumencor Sola Light Engine, a Lumenera 8MP Infinity3 Camera, a Zeiss GFP fluorescence filter set to 38 HE, and a Zeiss A-Plan 40× N.A. 0.55 objective. For each chamber in the glass slide, three sections of each film were randomly selected to quantify the bacterial attachment. Each attachment assay was performed on a minimum of three separate overnight bacterial cultures.

For the quantification of the bacterial cell number and surface area coverage, each image was first converted to a binary image using the threshold function of ImageJ (version 1.52q, National Institutes of Health), adjusting the threshold levels to maximize the isolation of individual cells and further segregating cell aggregates using the watershed function. These operations produced a binary image suitable for automated counting using the analyze particles function, with a count-size setting of 25 pixel² to infinity in order to prevent the counting of noise or sub-bacteria-sized debris. This analyze particles function provided as an output the total cell number per image and the area of the image occupied by each cell. The cell number was reported directly from the analyze particles function as the cell count. The bacterial coverage was calculated as the ratio of image area covered by all bacteria to the total image surface area.

Only live bacteria show GFP signals which can be observed using a fluorescence microscope. Significant differences between different samples were determined with an unpaired Student's t-test. Significance is denoted in graphs.

RESULTS

Effect of Polymer Film Coating on Bacterial Adhesion. Different polymers were applied to prepare the corresponding copolymer and homopolymer films through a facile evaporation method. Briefly, a fixed concentration of polymer solution was obtained by dissolving the polymer with specific solvents. Then, the prepared polymer solutions were evenly distributed into the chamber slides and completely dried to form the thin films on the substrate. These films were then tested for inhibition of early-stage bacterial attachment.

Cultures of fluorescent *P. aeruginosa* were chosen as the target bacteria, and the cell attachment was assessed by fluorescence microscopy. Generally, the fluorescence microscopic images indicated that no significant bacterial aggregates were formed on the surface of polymer films or the blank substrate (control) due to the limited incubation time; instead attachment and initial monolayer formation are observed. Figure 1 shows the pervasive distribution of bacteria on the surface of the blank; thousands of cells attached with a high surface coverage after the 15 min incubation period. This was expected as *P. aeruginosa* is known to initiate biofilm formation

on surfaces such as glass extremely quickly. These monolayers, left untreated, would develop into robust three-dimensional (3D) antibiotic-resistant biofilms over time.²²

The extent of attachment of fluorescent *P. aeruginosa* in wells coated with the polymer films was found dependent on the nature of the corresponding polymers. Significantly fewer fluorescent bacteria were observed on the surface of PS-PMAA, PS-PEO, and PS-PAA films compared with those on the blank glass substrate. These results indicate that the copolymer coating can effectively reduce the initial bacterial attachment. In contrast to the copolymer films, the homopolymer films exhibited much higher levels of bacterial attachment. Bacterial attachment to PMAA films was comparable with the blank. We observed reduced attachment to PMMA films in comparison with the blank, but this film facilitated significantly higher attachment than the copolymer films. These data indicate that there is a significant difference in resisting bacterial adhesion between copolymer films and homopolymer films.

These observations were further confirmed by quantitative analysis of the fluorescence images. As illustrated in Figure 2 and summarized in Table 1, bacterial attachment on all polymer films is significantly less than that on the blank substrate, as analyzed by both total fluorescence (count of bacteria on the surface) and surface area coverage. Of note, the surfaces coated with PS-PMAA reduced the number of attached bacteria by more than 99%, with a surface area coverage of less than 0.1%, in comparison with the blank, indicating excellent antifouling behavior. Similarly, PS-PEO and PS-PAA films also decreased the bacterial attachment up to 97 and 93%, respectively, as compared to the blank, each with a total surface area coverage of less than 2%. The PMMA films also showed a reduction in bacterial adhesion as compared to the blank, although they exhibited slightly more adhesion than the copolymer films, with a coverage of about 5%. As expected, analysis of PMAA films in comparison to the blank indicated only ~40% reduction in attached bacteria with a surface area coverage of 18%, which was close to that of the blank substrate. Although cell adhesion to PMAA is significantly lower than that on the control, it is also significantly higher than attachment to the copolymer films. This indicates that the copolymer films are significantly more effective in resisting bacterial adhesion. We hypothesized that this may result from structural characteristics or surface morphology differences in the copolymer films. Thus, a series of experiments were carried out to evaluate the surface

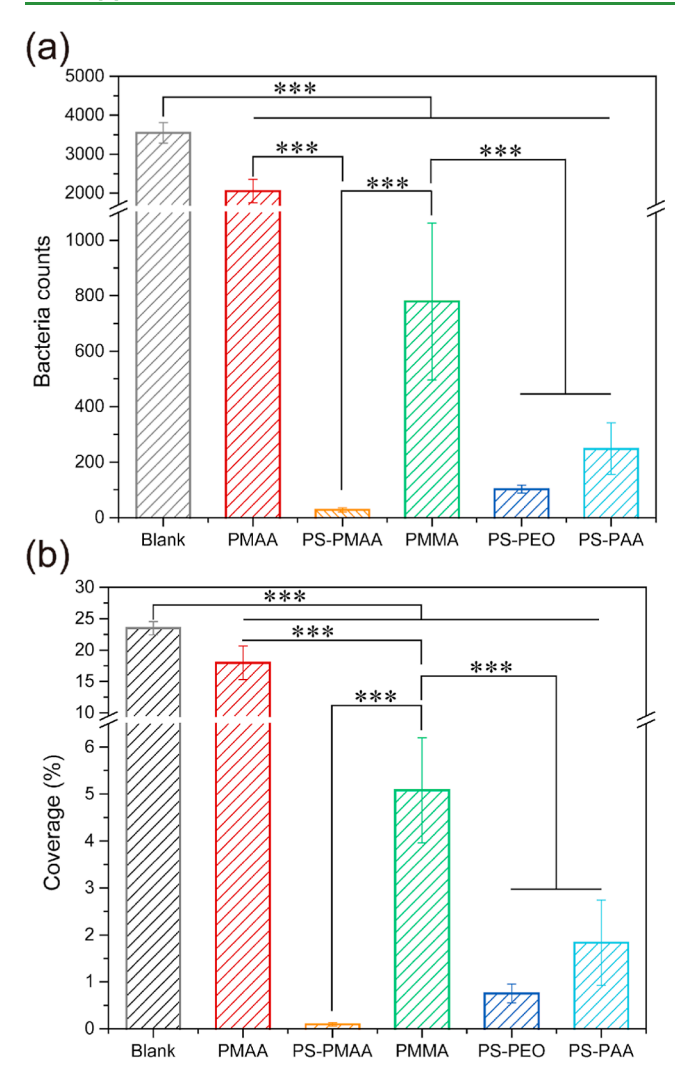


Figure 2. Summary of bacterial attachment on the blank and all polymer films for the number (a) and area coverage (b) of attached cells. A break is inserted in the y axis for better comparison of copolymer films and the blank. *** Statistically significant difference: p < 0.001 (unpaired Student's t-test).

properties of polymer films to determine the main factors that influence the bacterial adhesion.

Characterization of Polymer Film Surfaces. To understand the underlying mechanism of bacterial resistance of polymer films, the surface morphology was first characterized by AFM topographic analysis. As shown in Figure 3, the surface topography of different polymer films within a 5×5 μm^2 scan area varies considerably. Basically, the surface of homopolymer films appeared relatively smooth and uniform at the microscale, while the copolymer films exhibited significantly rough and inhomogeneous surfaces. Specifically, the surface roughness (R_q) of PS-PMAA films is 28.4 nm, which is much higher than that of any other polymer films. Examination of the 3D profiles of PS-PMAA films revealed the universal existence of spiky nanostructures on the surface. As for the PS-

PAA and PS-PEO copolymer films, uneven surfaces with relatively high surface roughness ($R_{\rm q}=14.1$ and 10.8 nm, respectively) were confirmed, which also contained nanoscale structures on the surface. This may also be associated with the similar performances in resisting bacterial attachment. However, no apparent peaks or sharp structures were observed on homopolymer PMAA films, which displayed relatively low surface roughness ($R_{\rm q}=1.40$ nm). For PMMA films, a flat and smooth surface morphology was also observed with low roughness ($R_{\rm q}=3.24$ nm). Such distinct surface properties in the nanoscale topography of copolymer films may result in great potential in prohibiting bacterial attachment by physicomechanical effects. ^{39,40,43}

In order to explore the role of surface nanoarchitecture of polymer films in the antifouling activity, the AFM crosssectional line profiles and other surface parameters including skewness and surface area difference were also derived from the AFM topographical analysis. In Figure 4 and Table 2, surface line profiles of PS-PMAA films confirmed the existence of numerous sharp peaks spaced at 30-50 nm, with most being in the height range from 20 to 80 nm. Similarly, PS-PEO and PS-PAA films were also found to display some sharp nanoneedles in the profiles, but with lower height and density. PMMA films were found to be mainly smooth surfaces other than a few peaks around 10 nm in height. When it comes to PMAA films, no significant peaks were detected, exhibiting a relatively even surface at the microscale. Figure 5 shows the peak distributions for all polymer films, which highlights the differences between all samples. A relatively narrow and symmetric peak distribution was observed on PMAA film surfaces, and most peaks or irregularities on PMAA surfaces were within the height of 5 nm, which verifies the existence of smooth and flat surfaces for these homopolymers. However, other polymer films show a broader peak distribution, especially for those copolymer films. Specifically, PMMA and PS-PAA films included some peaks in the height range from 10 to 20 nm, and PS-PEO films showed higher peaks at 30-40 nm. Rather than other films with a symmetric peak distribution, PS-PMAA films showed an asymmetric distribution with a second peak in the height range from 20 to 80 nm, which finally resulted in the nonuniform and spiky nanoarchitectures on the surface. Interestingly, all the peak distributions of polymer films conformed to a Gaussian distribution (Figure S2). This indicates that these peaks are normally distributed on the surface with a specific range, regardless of the composition of films, which were formed without complex processing methods. Such self-formed morphology on the surface may be related to the rearrangement of polymer chains during the drying process. Considering the difference between the copolymer PS-PMAA and homopolymer PMAA is the presence of polystyrene blocks, during the fabrication process, the hydrophobic PS blocks may form the observed sharp nanostructures on the surface. This may also be occurring in the other two copolymers with PS blocks (PS-PEO and PS-PAA), whose films also possessed such needle-like peaks, although not the same peak density and

Table 1. Summary of Bacterial Attachment to Polymer Films

	blank	PMAA	PS-PMAA	PMMA	PS-PEO	PS-PAA
bacterial count	3548 ± 262	2051 ± 298	27 ± 7	779 ± 282	102 ± 14	248 ± 93
coverage (%)	23.51 ± 1.06	17.99 ± 2.68	0.09 ± 0.04	5.08 ± 1.12	0.75 ± 0.20	1.83 ± 0.91

ACS Applied Bio Materials www.acsabm.org Article

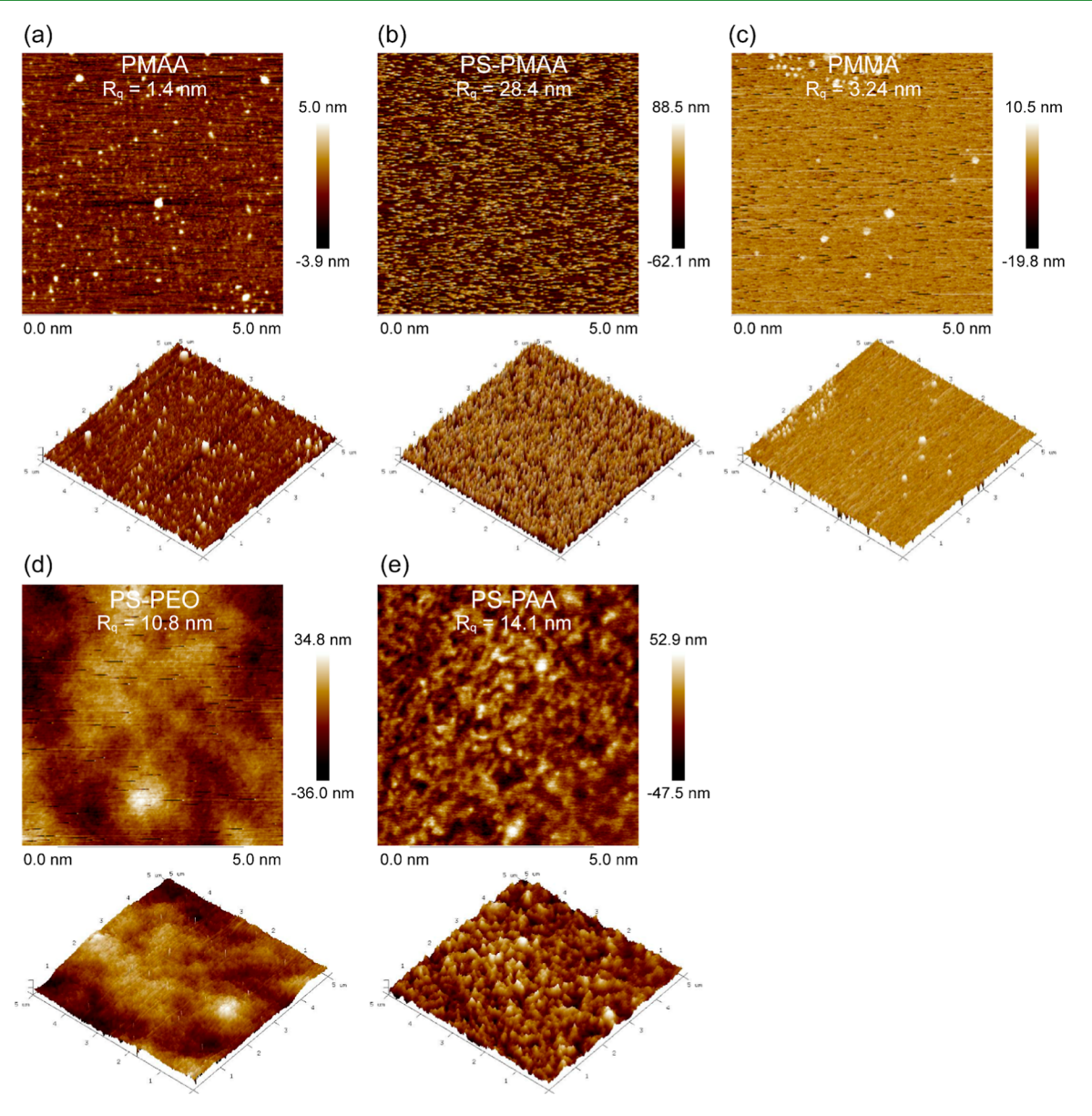


Figure 3. Surface topographies and the corresponding 3D AFM images of (a) PMAA, (b) PS-PMAA, (c) PMMA, (d) PS-PEO, and (e) PS-PAA. Image dimensions: $5 \times 5 \mu m$.

height. The relatively smooth and uniform surface of homopolymer PMMA films without PS blocks supports this.

The comparative analysis of the surface morphology based on the skewness parameters and surface area difference is shown in Table 2. Basically, the skewness parameter (S_{skw}) describes the asymmetry of the surface height distribution based on the mean height plane. For example, a positive value means the peak distribution is skewed to the right side and correlated with high peaks, while a negative value suggests the existence of valleys and the peak range is skewed left. The skewness value of PS-PMAA is about 1.8, demonstrating the presence of a significant number of peaks on the surface, while all other polymer films have negative skewness that shows the near-symmetrical or left-skewed distribution with less sharp peaks. Moreover, the difference between the 3D surface area and the projected surface area is also calculated and the results confirmed the prominent distinction of surface morphology of all polymer films. It suggested that the PS-PMAA films with uneven and rugged morphology presented a large surface area

difference (39.2%), while all other films that have smaller area difference (<11%) implied a relatively flat and less-steep morphology.

As previous researchers have discussed, 29,44 the hydrophobicity of the surface is one of the most paramount properties that may affect the cell adhesion and growth. Therefore, WCA measurements were performed to evaluate the wettability of the polymer film surface. As shown in Figure 6, most polymer films show hydrophilic surfaces, among which the PMAA film shows the most hydrophilic surface with a significantly lower WCA of $18.92 \pm 1.06^{\circ}$. The contact angles were observed to be around 61.80 ± 1.83 and $70.52 \pm 9.90^{\circ}$ on the PS-PMAA films and PS-PEO films, while PMMA films are statistically higher ($86.35 \pm 3.03^{\circ}$). The surface of PS-PAA was found to be slightly hydrophobic with the significantly higher contact angle over 90° ($99.22 \pm 5.89^{\circ}$).

In addition, surface charge is also considered as a factor that may interfere with bacterial adhesion and migration due to the potential electrostatic interactions between the surfaces and

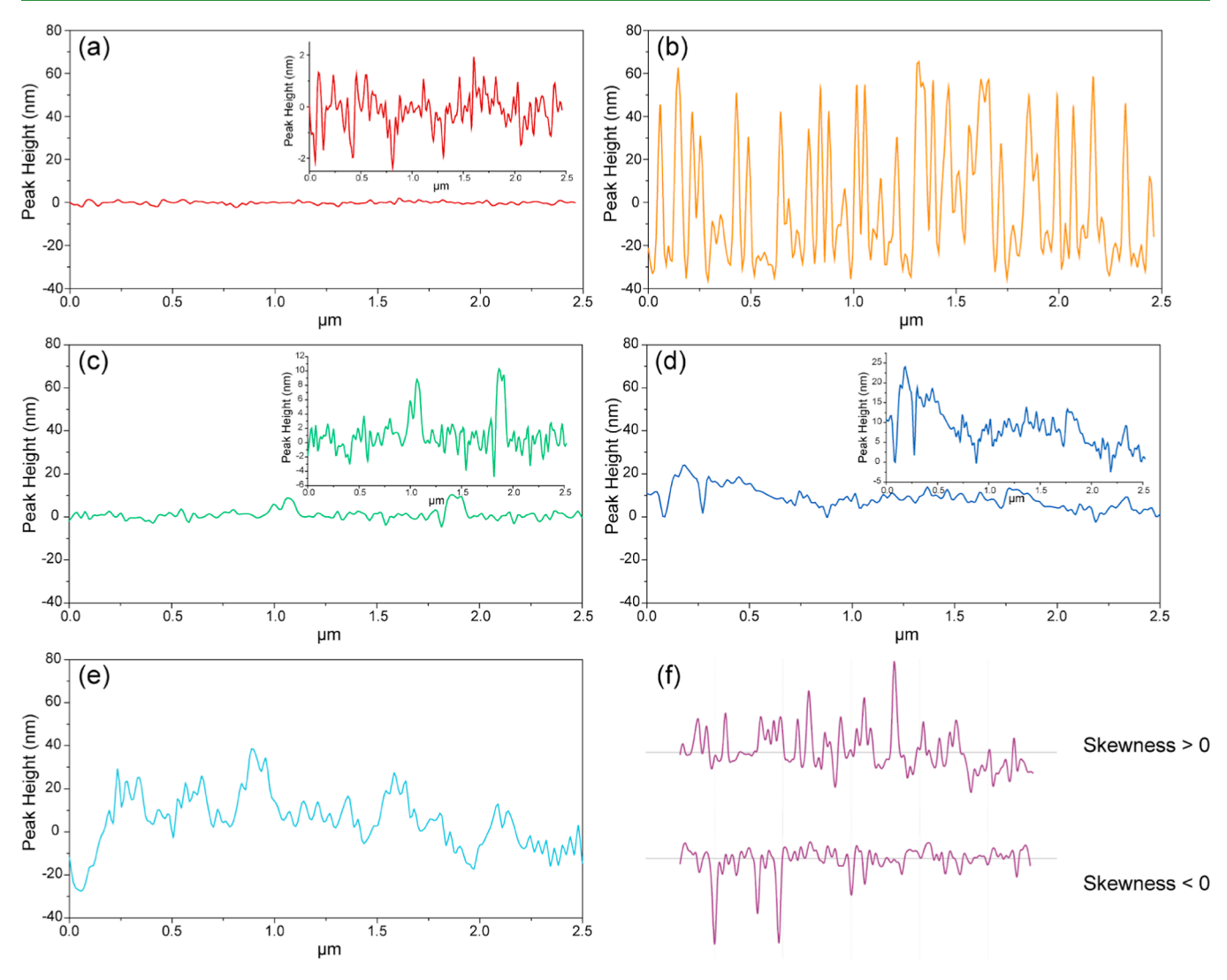


Figure 4. Representative AFM cross-sectional line profiles of (a) PMAA, (b) PS-PMAA, (c) PMMA, (d) PS-PEO, and (e) PS-PAA. (f) Reference to typical skewness profiles. The inset images present the line profiles in different height scales for better resolution.

Table 2. AFM Surface Roughness Analysis of All Polymer Film Surfaces

polymer	R_a (nm)	$\binom{R_q}{(nm)}$	$R_{\rm max} \choose {\rm nm}$	skewness $S_{ m skw}$	surface area difference (%)
PS-PMAA	24.5	28.4	92.1	1.8	39.2
PMAA	0.753	1.40	34.8	-1.6	0.5
PMMA	1.72	3.24	54.3	-4.0	3.4
PS-PEO	8.46	10.8	188	-4.4	10.6
PS-PAA	11.2	14.1	52.8	-0.6	5.4

cells.⁴⁵ We examined the surface potentials of thin polymer films by KFM. Generally, the surface potential images in Figure 7 show all the surfaces with the similar profiles of potential. Both the potential range and the potential distribution exhibit similar trends regardless of polymer components, and the potential values lie within the range from -20 to 20 mV (Figure S3). We also investigated zeta potentials of the corresponding polymer solution (Figure S4), which varied remarkably between different polymers. Such a huge discrepancy between surface potential and zeta potential of the solution may be related to the different ability of attraction of counterions by polymer chains in the solution, which

resulted in the various zeta potential values instead of similar surface potentials.

Effect of the Addition of Polymer Solutions on Bacterial Adhesion. In order to further verify that the physical nanostructures of the surfaces are impacting bacterial adhesion, rather than chemical characteristics of the polymers themselves, we dispensed the same amount of bacterial cultures directly into polymer solution without first depositing the film coating on the substrate. The same concentration of bacterial culture was used to keep the experimental conditions consistent. Figure 8 shows fluorescence images for all polymer solutions except for PMMA due to the insolubility of PMMA in the aqueous solution. The direct addition of bacterial culture into polymer solutions resulted in similar bacterial count and area coverage in all samples analyzed. This is distinctly different from the results obtained for bacterial deposition onto polymer-coated substrates. The fluorescence images revealed that cells were evenly distributed in the scan area for all the polymer solutions, and all polymer solutions showed similar bacterial adhesion compared with the blank samples. Considering the short duration of cell incubation, we do not expect extensive formation of multilayers of cells, in spite of the high bacterial count. Some overlapped or adherent bacteria

ACS Applied Bio Materials www.acsabm.org Article

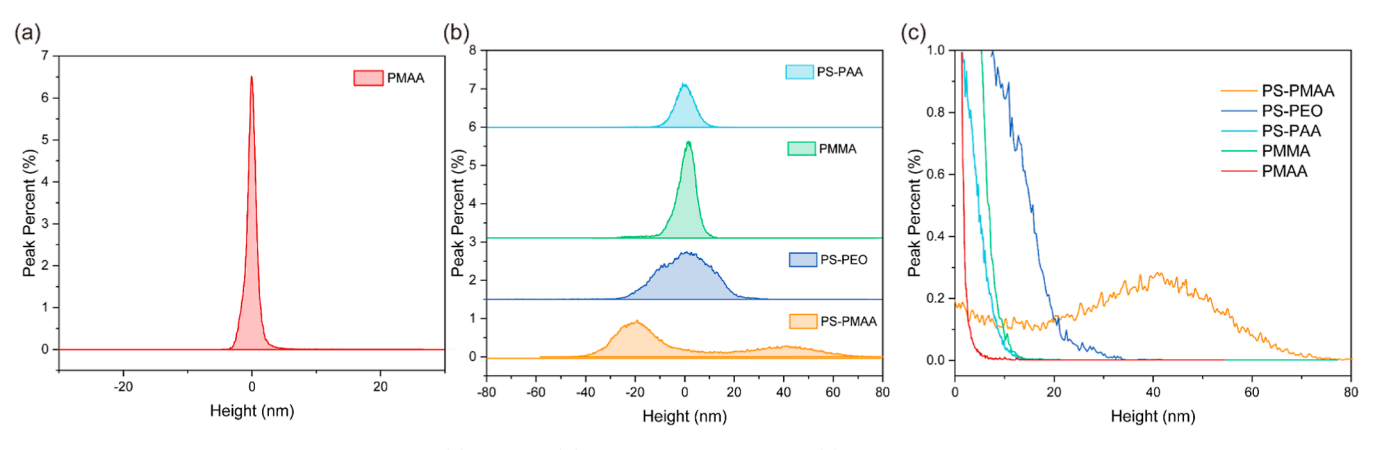


Figure 5. Peak distribution of polymer films: (a) PMAA, (b) all other polymers, and (c) peak distribution in the range from 0 to 80 nm in one percent scale. The percentage profiles of all polymers except PS-PMAA in (b) are shifted for better clarity.

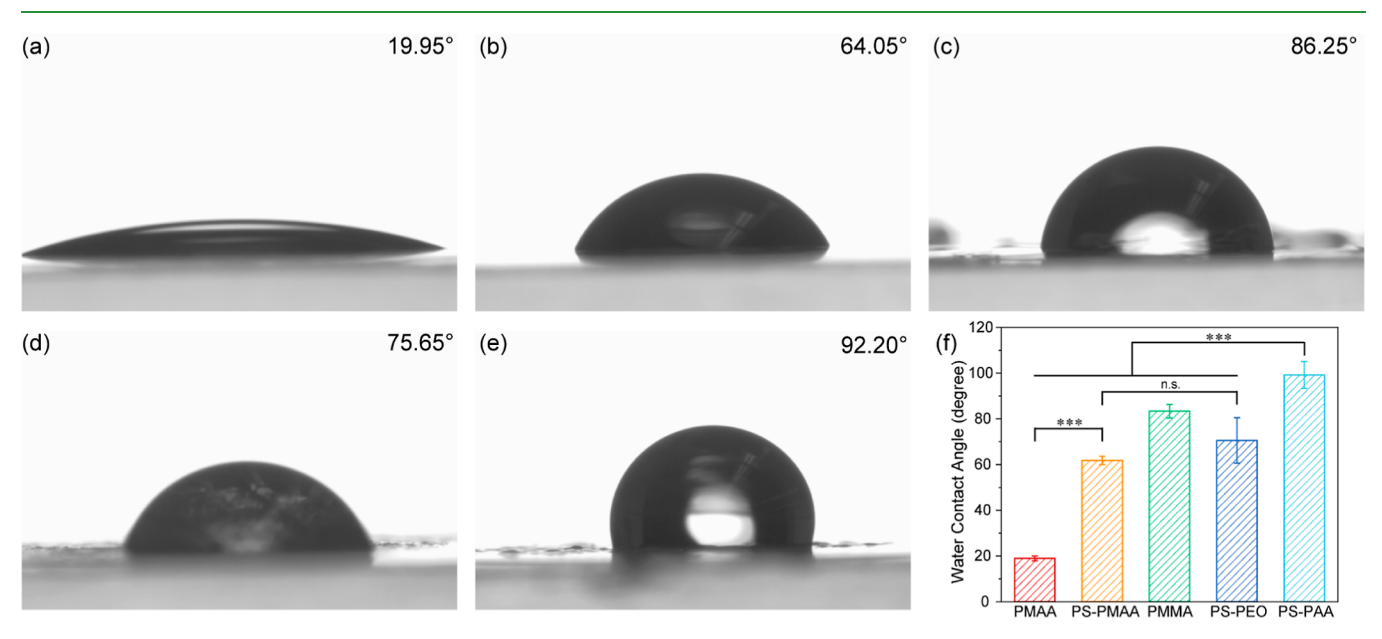


Figure 6. Representative snapshot images of the water droplet on polymer films: (a) PMAA, (b) PS-PMAA, (c) PMMA, (d) PS-PEO, and (e) PS-PAA. (f) Summary of static WCA measurements. *** Statistically significant difference: *p* < 0.001 (unpaired Student's *t*-test) and n.s. indicates no statistical significance.

appear in the fluorescence images; we believe these could be due to visual dislocation since some bacteria were suspended in the solution when images were taken overhead. These data are quantified in Figure 9 and summarized in Table 3. It is evident that all the copolymer solutions, including PS-PMAA, PS-PEO, and PS-PAA, only led to around 44% decrease at best, while the copolymer films achieved excellent resistance to the bacterial attachment, with over a 90% decrease in attached cells. For the homopolymer PMAA, the influence of the addition of polymer solution was comparable with that of the polymer film, but neither application of polymer resulted in remarkable resistance of bacterial attachment, in comparison with the blank. Overall, these data confirm our hypothesis that bacterial attachment is a function of surface topology.

DISCUSSION

P. aeruginosa is known as an intractable strain that can easily colonize the surfaces of medical and implant devices, such as ventilators and catheters, causing severe nosocomial infection. The resulting biofilm infections are extremely resistant to antibiotic treatment. Thus, there is a growing need to develop

novel approaches to inhibit bacterial adhesion and biofilm formation. Of particular interest to researchers are prophylactic and facile methods with direct action on the local surface that could effectively delay and even prevent the formation of bacterial biofilms.³⁹

Examination of our thin polymer films suggests that polymer surface morphology results in remarkable differences in the cell attachment and distribution. In general, the fluorescence images indicate that bacteria favor attachment to smooth and flat surfaces, such as the uncoated blank slide and PMAAcoated slides. Previous studies have indicated that flat surfaces could be beneficial to the movement and proliferation of motile bacteria such as P. aeruginosa. 46,47 Thus, we conclude that the existence of sharp peaks and inhomogeneous surface morphology, as verified by AFM, in some of our copolymer films hinders the attachment of cells, leading to low bacterial attachment and surface area coverage. The surface line profile and the positive skewness value also support the importance of nanoarchitecture on bacterial surface attachment. We propose that spiky or conical features on the order of 20-80 nm can inhibit the early stage of bacterial adhesion by direct contact.

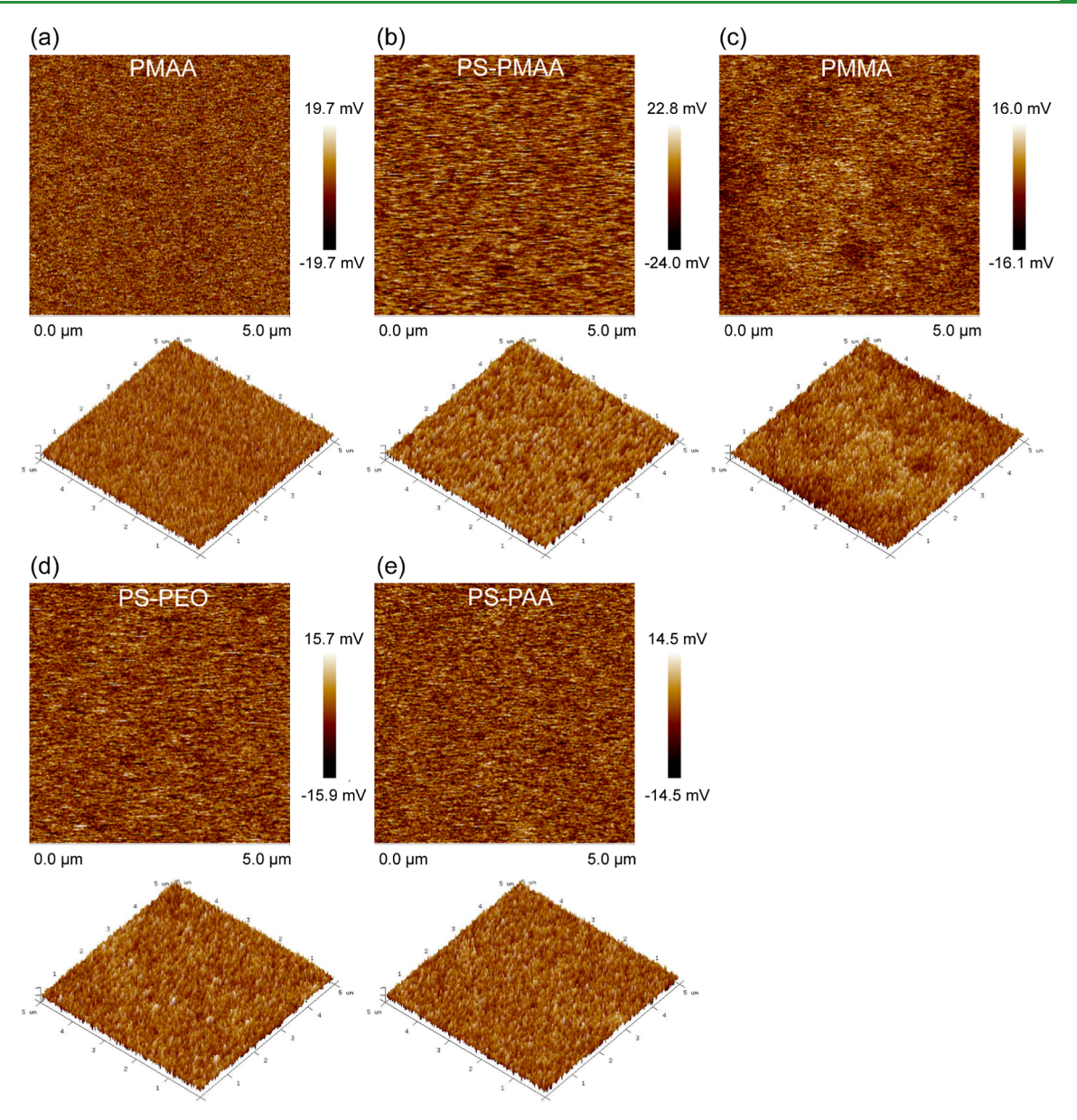


Figure 7. Surface potential and the corresponding 3D KFM images of (a) PMAA, (b) PS-PMAA, (c) PMMA, (d) PS-PEO, and (e) PS-PAA. Image dimensions: $5 \times 5 \mu m$.

Such uneven surface topography could limit the possible mobility and interactions between cells which in turn delay or restrain the bacterial growth and the following biofilm formation. Considering that P. aeruginosa is $1-2~\mu m$ in the length scale, the pressure exerted by nanoscale structures on contact may be able to penetrate the cell membrane and lead to cell death which may bring about the bactericidal action. By comparing the chemical structures of PMAA and PS-PMAA, the main cause for such different surface morphologies is related to the introduction of PS blocks in the copolymer chains, which remarkably increased the surface roughness and assisted to form the nanoscale patterns on the surface. In addition, the hydrophobic segments from the polymer network may also play a nontrivial role in the antifouling mechanism.

Although surface properties including surface hydrophobicity and surface potential are reported as the vital parameters in the antibacterial mechanism of antifouling surface, we find that the wettability and surface potential of coated surfaces may not

contribute as much to the antifouling function as other literature has suggested, ^{22,23} or may be less important than the surface topography. Previous studies revealed that the increasing hydrophobicity of the film surface resulted in the increasing antibacterial behavior due to the reduction of attachment.41 In this work, all the polymer films show hydrophilic or slightly hydrophobic surfaces. Although the fact that PMAA films with excellent wettability perform worst in resisting bacterial adhesion and the hydrophobic PS-PAA films resist significant cells attached on the surface is consistent with previous studies, the PS-PMAA and PS-PEO films which have moderate hydrophilicity actually showed lower bacterial attachment compared with other samples. This suggests that in our work, the increasing hydrophobicity of the film surface seems not to be correlated with the increasing antibacterial performance. This is also reported in previous research that suggests no direct relationship between the surface superhydrophobicity and antifouling functionality.⁴³ In this light,

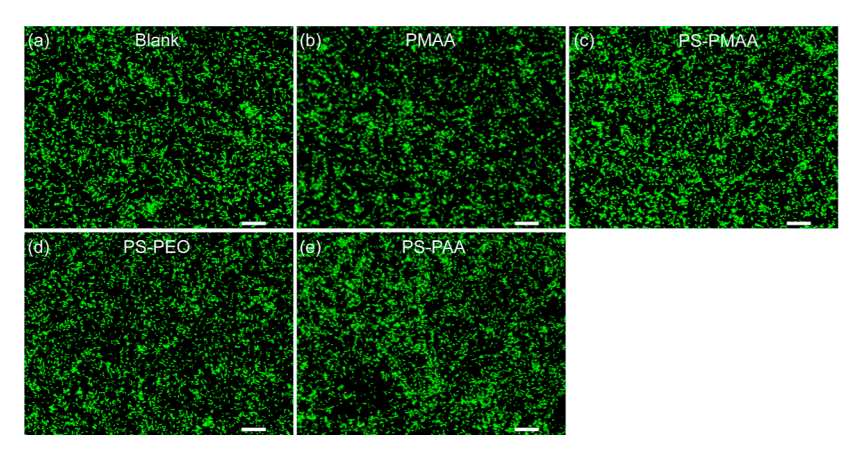


Figure 8. Representative fluorescence images of *P. aeruginosa* on the control and samples with the addition of polymer solutions: (a) blank, (b) PMAA, (c) PS-PMAA, (d) PS-PEO, and (e) PS-PAA. No result for PMMA solution due to the insolubility in aqueous solutions. The apparent overlapping of cells could be caused by the suspended cells in the polymer solution rather than the formation of multilayer colonies due to the overhead imaging. Scale bar: $20 \mu m$.

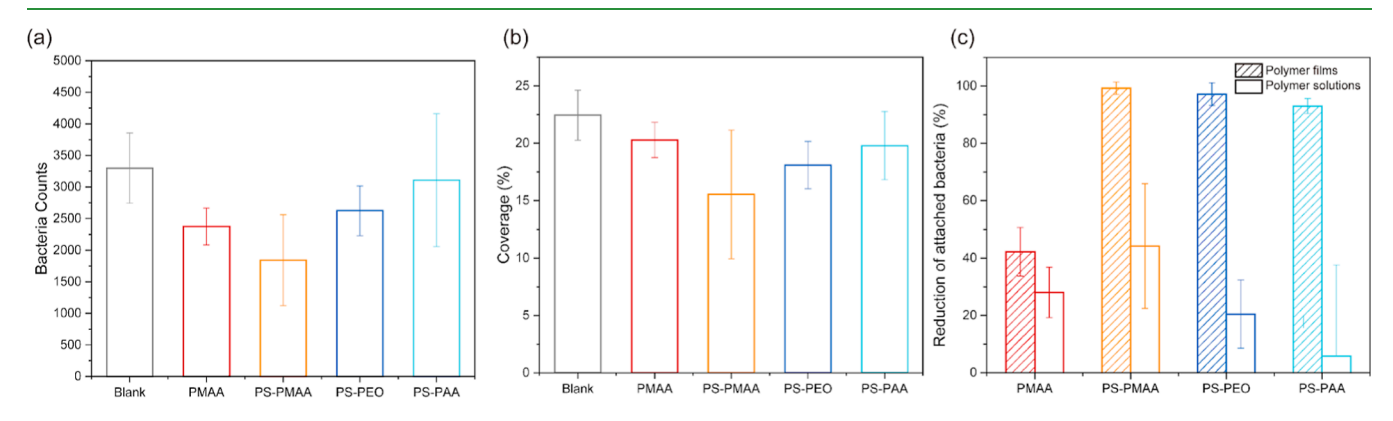
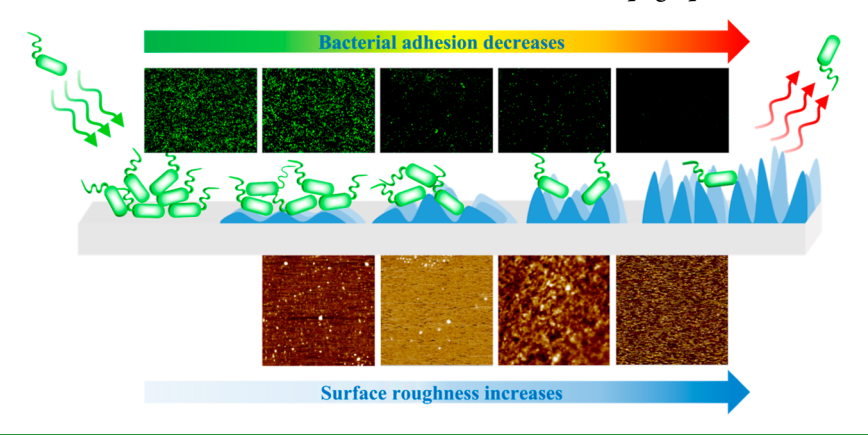


Figure 9. Summary of bacterial count on the blank and samples with the addition of polymer solutions for the number (a) and area coverage (b). (c) Comparison between polymer films and polymer solution in the reduction of attached bacteria.

Table 3. Summary of Bacterial Attachment on the Blank and Samples with the Addition of Polymer Solutions

	blank	PMAA	PS-PMAA	PMMA	PS-PEO	PS-PAA
bacterial count	3299 ± 555	2374 ± 289	1841 ± 717	N/A	2624 ± 392	3109 ± 1050
coverage (%)	22.44 ± 2.18	20.28 ± 1.54	15.55 ± 5.6	N/A	2374 ± 289	19.79 ± 2.97

Scheme 2. Schematic Illustration of Bacterial Adhesion on Different Surface Topographies



surface wettability may have some influences on bacterial adhesion but not be dominant to contribute to the prohibition of cell attachment. The KFM images also revealed similar potential mappings of all the samples which are not responsible for the varied bacterial attachment behavior. The comparison

of the surface potential of all the films is not sufficient to explain the different results of cell adhesion, and this could be excluded as an insignificant effect on the bacterial attachment in this work. Considering these uncorrelated or similar surface properties, it is reasonable to hypothesize that the differences in cell adhesion have to do with the physical structures of polymer film surfaces which show as nanoscale patterns and provide potential mechanical bactericidal effects (Scheme 2).

To better understand the significance of nanoscale physical structure on the film surface, we conducted further studies of bacterial attachment with the addition of polymer solutions. These experiments would demonstrate if any antibacterial activity was due to any inherent antibacterial properties or chemical characteristics of the polymers themselves. Bacterial attachment increased in both density and area coverage compared with the samples with predeposition of polymer films, which confirmed the suppression of physical surface structure on cell activities. Although most polymer solutions led to similar bacterial adhesion with the blank, the addition of PS-PMAA solution still displayed the highest bacterial resistance and lowest bacterial adhesion, which may come from the interactions between hydrophobic segments and cells with the potential penetration into cell membranes. However, all the samples still showed significantly higher adhesion except PMAA which showed similar results in both dried and solution states. In other words, the lack of physical structures with nanoscale patterns resulted in significantly diminished antibacterial effects, demonstrating that the self-formed nanostructured surface by drying is dominant in resisting bacterial adhesion, even though the chemical characteristics of the polymer chains may also have some influence.

Of note, the nanotextured surfaces that have been previously proposed for antibacterial and antifouling behavior are often fabricated using complex high-cost processes in order to create well-organized nanostructures or artificial biomimetic surfaces with superhydrophobicity in the aforementioned studies. However, in this work, only a facile evaporation approach to prepare copolymer films was applied. Considering these self-patterned films displayed excellent bacterial resistance, such an approach provides advantages over those counterparts due to not involving any complex postprocessing or chemical treatments, which is straightforward and convenient to perform without any specific requirements.

CONCLUSIONS

In summary, various thin polymer films, including homopolymer and copolymer components, were fabricated with a facile evaporation approach and then exposed to the bacterium P. aeruginosa to evaluate the potential influences on bacterial adhesion. A substantial amount of bacterial adhesion was observed on the surface of homopolymer PMAA films, while the bacterial count and surface area coverage were reduced significantly on the surface of copolymer PS-PMAA films. By examining the surface morphology of polymer films, it was found that the patterned nanostructures on the film surfaces hindered the bacterial adhesion with spiky peaks in nanoscale, which possess the capacity to inactivate the bacteria upon direct contact. After the exploration of related surface properties including hydrophobicity and surface potential, it is believed that the nanoarchitectural physical structures of the polymer film surface are primarily responsible for resisting the bacterial adhesion, potentially through mechano-bactericidal action. This suggests that the random surface topography could potentially affect or inhibit bacterial fouling on the surfaces of common materials and that elaborate design of well-ordered topographic structures is not necessarily required to create surfaces that resist bacterial adhesion. This work provides an economic and environmentally friendly approach

to control bacterial contamination and biofilm formation and opens the possibility for the simple design and preparation of thin polymer films for other potential medical applications.

ASSOCIATED CONTENT

Solution Supporting Information

The Supporting Information is available free of charge at https://pubs.acs.org/doi/10.1021/acsabm.2c00416.

Chemical structures of all polymers, KFM profiles of all polymer films, fits to Gaussian distributions of peaks from AFM data for all polymer films, and zeta potential measurements of polymer solutions (PDF)

AUTHOR INFORMATION

Corresponding Author

Surita R. Bhatia — Department of Chemistry, Stony Brook University, Stony Brook, New York 11794-3400, United States; orcid.org/0000-0002-5950-193X; Email: surita.bhatia@stonybrook.edu

Authors

Jiachun Shen – Department of Chemistry, Stony Brook University, Stony Brook, New York 11794-3400, United States

Danielle Guercio – Department of Chemistry, Stony Brook University, Stony Brook, New York 11794-3400, United States

Ilana L. Heckler – Department of Chemistry, Stony Brook University, Stony Brook, New York 11794-3400, United States

Ting Jiang — Department of Chemistry, Stony Brook University, Stony Brook, New York 11794-3400, United States; orcid.org/0000-0001-5349-3396

Scott T. Laughlin – Department of Chemistry, Stony Brook University, Stony Brook, New York 11794-3400, United States; Occid.org/0000-0002-9134-1200

Elizabeth M. Boon — Department of Chemistry, Stony Brook University, Stony Brook, New York 11794-3400, United States; orcid.org/0000-0003-1891-839X

Complete contact information is available at: https://pubs.acs.org/10.1021/acsabm.2c00416

Notes

The authors declare no competing financial interest.

ACKNOWLEDGMENTS

Financial support for this work was provided by NSF awards CBET-1903189 and DGE-1922639, NIH awards GM118894 (to E.M.B.) and T32GM136572 (to I.L.H.), and a Stony Brook University Office of the Vice President for Research (OVPR) Seed Grant. The sponsors had no role in the study design; in the collection, analysis, and interpretation of data; in the writing of the report; and in the decision to submit the article for publication.

REFERENCES

- (1) Donlan, R. M. Biofilms and device-associated infections. *Emerging Infect. Dis.* **2001**, *7*, 277–281.
- (2) VanEpps, J. S.; Younger, J. G. Implantable Device-Related Infection. *Shock* **2016**, *46*, 597–608.
- (3) Park, D. R. The microbiology of ventilator-associated pneumonia. *Respir. Care* **2005**, *50*, 742–563.

- (4) Berne, C.; Ellison, C. K.; Ducret, A.; Brun, Y. V. Bacterial adhesion at the single-cell level. *Nat. Rev. Microbiol.* **2018**, *16*, 616–627.
- (5) Jamal, M.; Ahmad, W.; Andleeb, S.; Jalil, F.; Imran, M.; Nawaz, M. A.; Hussain, T.; Ali, M.; Rafiq, M.; Kamil, M. A. Bacterial biofilm and associated infections. *J. Chin. Med. Assoc.* **2018**, *81*, 7–11.
- (6) Busscher, H. J.; van der Mei, H. C.; Subbiahdoss, G.; Jutte, P. C.; van den Dungen, J. J.; Zaat, S. A.; Schultz, M. J.; Grainger, D. W. Biomaterial-associated infection: locating the finish line in the race for the surface. *Sci. Transl. Med.* **2012**, *4*, 153rv10.
- (7) Stewart, P. S.; William Costerton, J. W. Antibiotic resistance of bacteria in biofilms. *Lancet* **2001**, *358*, 135–138.
- (8) Tenover, F. C. Mechanisms of antimicrobial resistance in bacteria. *Am. J. Med.* **2006**, *119*, S3–S10.
- (9) Abadi, A. T. B.; Rizvanov, A. A.; Haertlé, T.; Blatt, N. L. World Health Organization report: current crisis of antibiotic resistance. *BioNanoScience* **2019**, *9*, 778–788.
- (10) Cui, Q.; Liu, T.; Li, X.; Song, K.; Ge, D. Nanopillared Polycarbonate Surfaces Having Variable Feature Parameters as Bactericidal Coatings. ACS Appl. Nano Mater. 2020, 3, 4599–4609.
- (11) Arias, S. L.; Devorkin, J.; Spear, J. C.; Civantos, A.; Allain, J. P. Bacterial Envelope Damage Inflicted by Bioinspired Nanostructures Grown in a Hydrogel. ACS Appl. Bio Mater. 2020, 3, 7974–7988.
- (12) Kargar, M.; Chang, Y.-R.; Khalili Hoseinabad, H.; Pruden, A.; Ducker, W. A. Colloidal crystals delay formation of early stage bacterial biofilms. *ACS Biomater. Sci. Eng.* **2016**, *2*, 1039–1048.
- (13) Park, S.-M.; Kim, D.-A.; Jo, J.-K.; Jun, S.-K.; Jang, T.-S.; Kim, H.-W.; Lee, J.-H.; Lee, H.-H. Ceria-Incorporated Biopolymer for Preventing Fungal Adhesion. *ACS Biomater. Sci. Eng.* **2020**, *7*, 1808–1816
- (14) Wu, Q.; Peng, R.; Luo, Y.; Cui, Q.; Zhu, S.; Li, L. Antibacterial Activity of Porous Gold Nanocomposites via NIR Light-Triggered Photothermal and Photodynamic Effects. *ACS Appl. Bio Mater.* **2021**, *4*, 5071–5079.
- (15) Fernandes, T. A.; Costa, I. F.; Jorge, P.; Sousa, A. C.; André, V.; Cerca, N.; Kirillov, A. M. Silver(I) Coordination Polymers Immobilized into Biopolymer Films for Antimicrobial Applications. ACS Appl. Mater. Interfaces 2021, 13, 12836–12844.
- (16) Häffner, S. M.; Nyström, L.; Browning, K. L.; Mörck Nielsen, H.; Strömstedt, A. A.; Van Der Plas, M. J.; Schmidtchen, A.; Malmsten, M. Interaction of laponite with membrane components—consequences for bacterial aggregation and infection confinement. ACS Appl. Mater. Interfaces 2019, 11, 15389—15400.
- (17) Yang, S.; Tran, C.; Whiteley, G. S.; Glasbey, T.; Kriel, F. H.; McKenzie, D. R.; Manos, J.; Das, T. Covalent Immobilization of N-Acetylcysteine on a Polyvinyl Chloride Substrate Prevents Bacterial Adhesion and Biofilm Formation. *Langmuir* **2020**, *36*, 13023–13033.
- (18) Francius, G.; Cervulle, M.; Clément, E.; Bellanger, X.; Ekrami, S.; Gantzer, C.; Duval, J. F. Impacts of Mechanical Stiffness of Bacteriophage-Loaded Hydrogels on Their Antibacterial Activity. *ACS Appl. Bio Mater.* **2021**, *4*, 2614–2627.
- (19) Wei, G.; Nguyen, D.; Reghu, S.; Li, J.; Chua, C.; Ishida, Y.; Chan-Park, M. B. Fast-bactericidal effect of polyion complex nanoparticles on gram-negative bacteria. *ACS Appl. Nano Mater.* **2020**, *3*, 2654–2664.
- (20) Druvari, D.; Koromilas, N. D.; Lainioti, G. C.; Bokias, G.; Vasilopoulos, G.; Vantarakis, A.; Baras, I.; Dourala, N.; Kallitsis, J. K. Polymeric quaternary ammonium-containing coatings with potential dual contact-based and release-based antimicrobial activity. *ACS Appl. Mater. Interfaces* **2016**, *8*, 35593–35605.
- (21) Chen, Q.; Yu, S.; Zhang, D.; Zhang, W.; Zhang, H.; Zou, J.; Mao, Z.; Yuan, Y.; Gao, C.; Liu, R. Impact of antifouling PEG layer on the performance of functional peptides in regulating cell behaviors. *J. Am. Chem. Soc.* **2019**, *141*, 16772–16780.
- (22) Ghilini, F.; Pissinis, D. E.; Miñán, A.; Schilardi, P. L.; Diaz, C. How functionalized surfaces can inhibit bacterial adhesion and viability. *ACS Biomater. Sci. Eng.* **2019**, *5*, 4920–4936.
- (23) Ivanova, E. P.; Hasan, J.; Webb, H. K.; Truong, V. K.; Watson, G. S.; Watson, J. A.; Baulin, V. A.; Pogodin, S.; Wang, J. Y.; Tobin, M.

- J.; Löbbe, C.; Crawford, R. J. Natural bactericidal surfaces: mechanical rupture of Pseudomonas aeruginosa cells by cicada wings. *Small* **2012**, *8*, 2489–2494.
- (24) Kelleher, S. M.; Habimana, O.; Lawler, J.; O' Reilly, B.; Daniels, S.; Casey, E.; Cowley, A. Cicada wing surface topography: an investigation into the bactericidal properties of nanostructural features. ACS Appl. Mater. Interfaces 2016, 8, 14966–14974.
- (25) Dundar Arisoy, F.; Kolewe, K. W.; Homyak, B.; Kurtz, I. S.; Schiffman, J. D.; Watkins, J. J. Bioinspired photocatalytic shark-skin surfaces with antibacterial and antifouling activity via nanoimprint lithography. ACS Appl. Mater. Interfaces 2018, 10, 20055–20063.
- (26) Jiang, R.; Hao, L.; Song, L.; Tian, L.; Fan, Y.; Zhao, J.; Liu, C.; Ming, W.; Ren, L. Lotus-leaf-inspired hierarchical structured surface with non-fouling and mechanical bactericidal performances. *Chem. Eng. J.* **2020**, 398, 125609.
- (27) Koch, K.; Bhushan, B.; Jung, Y. C.; Barthlott, W. Fabrication of artificial Lotus leaves and significance of hierarchical structure for superhydrophobicity and low adhesion. *Soft Matter* **2009**, *5*, 1386–1393.
- (28) Le, P. H.; Nguyen, D. H.; Aburto-Medina, A.; Linklater, D. P.; Crawford, R. J.; MacLaughlin, S.; Ivanova, E. P. Nanoscale Surface Roughness Influences Candida albicans Biofilm Formation. *ACS Appl. Bio Mater.* **2020.** 3, 8581–8591.
- (29) Cao, Y.; Jana, S.; Bowen, L.; Tan, X.; Liu, H.; Rostami, N.; Brown, J.; Jakubovics, N. S.; Chen, J. Hierarchical rose petal surfaces delay the early-stage bacterial biofilm growth. *Langmuir* **2019**, *35*, 14670–14680.
- (30) Xu, L.-C.; Siedlecki, C. A. Submicron-textured biomaterial surface reduces staphylococcal bacterial adhesion and biofilm formation. *Acta Biomater.* **2012**, *8*, 72–81.
- (31) Kargar, M.; Pruden, A.; Ducker, W. A. Preventing bacterial colonization using colloidal crystals. *J. Mater. Chem. B* **2014**, *2*, 5962–5971.
- (32) Fisher, L. E.; Yang, Y.; Yuen, M.-F.; Zhang, W.; Nobbs, A. H.; Su, B. Bactericidal activity of biomimetic diamond nanocone surfaces. *Biointerphases* **2016**, *11*, 011014.
- (33) Heckmann, T. S.; Schiffman, J. D. Spatially Organized Nanopillar Arrays Dissimilarly Affect the Antifouling and Antibacterial Activities of Escherichia coli and Staphylococcus aureus. *ACS Appl. Nano Mater.* **2019**, *3*, 977–984.
- (34) Linklater, D. P.; Nguyen, H. K. D.; Bhadra, C. M.; Juodkazis, S.; Ivanova, E. P. Influence of nanoscale topology on bactericidal efficiency of black silicon surfaces. *Nanotechnology* **2017**, *28*, 245301.
- (35) Valiei, A.; Lin, N.; Bryche, J.-F.; McKay, G.; Canva, M.; Charette, P. G.; Nguyen, D.; Moraes, C.; Tufenkji, N. Hydrophilic mechano-bactericidal nanopillars require external forces to rapidly kill bacteria. *Nano Lett.* **2020**, *20*, 5720–5727.
- (36) Hazell, G.; Fisher, L. E.; Murray, W. A.; Nobbs, A. H.; Su, B. Bioinspired bactericidal surfaces with polymer nanocone arrays. *J. Colloid Interface Sci.* **2018**, 528, 389–399.
- (37) Ma, J.; Sun, Y.; Gleichauf, K.; Lou, J.; Li, Q. Nanostructure on taro leaves resists fouling by colloids and bacteria under submerged conditions. *Langmuir* **2011**, *27*, 10035–10040.
- (38) Shahali, H.; Hasan, J.; Mathews, A.; Wang, H.; Yan, C.; Tesfamichael, T.; Yarlagadda, P. K. Multi-biofunctional properties of three species of cicada wings and biomimetic fabrication of nanopatterned titanium pillars. *J. Mater. Chem. B* **2019**, *7*, 1300–1310.
- (39) Linklater, D. P.; Baulin, V. A.; Juodkazis, S.; Crawford, R. J.; Stoodley, P.; Ivanova, E. P. Mechano-bactericidal actions of nanostructured surfaces. *Nat. Rev. Microbiol.* **2021**, *19*, 8–22.
- (40) Ivanova, E. P.; Hasan, J.; Webb, H. K.; Gervinskas, G.; Juodkazis, S.; Truong, V. K.; Wu, A. H.; Lamb, R. N.; Baulin, V. A.; Watson, G. S.; Watson, J. A.; Mainwaring, D. E.; Crawford, R. J. Bactericidal activity of black silicon. *Nat. Commun.* **2013**, *4*, 2838.
- (41) Lu, Y.; Wu, Y.; Liang, J.; Libera, M. R.; Sukhishvili, S. A. Self-defensive antibacterial layer-by-layer hydrogel coatings with pH-triggered hydrophobicity. *Biomaterials* **2015**, *45*, 64–71.

- (42) Whitmire, J. M.; Merrell, D. S. Successful culture techniques for Helicobacter species: general culture techniques for Helicobacter pylori. *Helicobacter Species*; Springer, 2012; pp 17–27.
- (43) Ishantha Senevirathne, S.; Hasan, J.; Mathew, A.; Jaggessar, A.; Yarlagadda, P. K. Trends in Bactericidal Nanostructured Surfaces: An Analytical Perspective. *ACS Appl. Bio Mater.* **2021**, *4*, 7626–7642.
- (44) Zhang, S.; Liang, X.; Gadd, G. M.; Zhao, Q. Superhydrophobic coatings for urinary catheters to delay bacterial biofilm formation and catheter-associated urinary tract infection. *ACS Appl. Bio Mater.* **2019**, 3, 282–291.
- (45) Campoccia, D.; Montanaro, L.; Arciola, C. R. A review of the biomaterials technologies for infection-resistant surfaces. *Biomaterials* **2013**, *34*, 8533–8554.
- (46) Chang, Y.-R.; Weeks, E. R.; Barton, D.; Dobnikar, J.; Ducker, W. A. Effect of topographical steps on the surface motility of the bacterium pseudomonas aeruginosa. *ACS Biomater. Sci. Eng.* **2019**, *5*, 6436–6445.
- (47) Chang, Y.-R.; Weeks, E. R.; Ducker, W. A. Surface topography hinders bacterial surface motility. ACS Appl. Mater. Interfaces 2018, 10, 9225—9234
- (48) Ivanova, E. P.; Linklater, D. P.; Werner, M.; Baulin, V. A.; Xu, X.; Vrancken, N.; Rubanov, S.; Hanssen, E.; Wandiyanto, J.; Truong, V. K.; Elbourne, A.; Maclaughlin, S.; Juodkazis, S.; Crawford, R. J. The multi-faceted mechano-bactericidal mechanism of nanostructured surfaces. *Proc. Natl. Acad. Sci. U.S.A.* **2020**, *117*, 12598–12605.

☐ Recommended by ACS

Submicrometer-Sized Roughness Suppresses Bacteria Adhesion

Noemí Encinas, Doris Vollmer, et al.

MARCH 06, 2020

ACS APPLIED MATERIALS & INTERFACES

READ 🗹

Zinc Oxide Superstructures in Colloidal Polymer Nanocomposite Films: Enhanced Antibacterial Activity through Slow Drying

Yichen Dong, Ignacio Martín-Fabiani, et al.

JANUARY 08, 2020

ACS APPLIED POLYMER MATERIALS

READ 🗹

Flexible Hierarchical Wraps Repel Drug-Resistant Gram-Negative and Positive Bacteria

Sara M. Imani, Leyla Soleymani, et al.

DECEMBER 13, 2019

ACS NANO

READ [7

Non-leaching, Highly Biocompatible Nanocellulose Surfaces That Efficiently Resist Fouling by Bacteria in an Artificial Dermis Model

Ghada Hassan, Vânia M. Moreira, et al.

JUNE 13, 2020

ACS APPLIED BIO MATERIALS

READ 🗹

Get More Suggestions >